DALTON
FULL PAPER

Effect of thermal annealing on the ferrimagnetic behavior and ordering of the $[MnTXPP]^{+}[TCNE]^{\bullet -}\cdot$solv (X = F, Cl, Br, I; solv = PhMe, CH_2Cl_2) family of magnets †

Durrell K. Rittenberg, Atta M. Arif and Joel S. Miller *

Department of Chemistry, 315 S. 1400 E. RM 2124, Salt Lake City, UT 84112-0850, USA. E-mail: jsmiller@chemistry.utah.edu

Received 2nd May 2000, Accepted 21st June 2000
First published as an Advance Article on the web 21st September 2000

5,10,15,20-Tetrakis(4-fluorophenyl)porphyrinatomanganese(III) tetracyanoethenide, [MnTFPP][TCNE], **1F**, 5,10,15,20-tetrakis(4-bromophenyl)porphyrinatomanganese(III) tetracyanoethenide, [MnTBrPP][TCNE], **1Br**, and 5,10,15,20-tetrakis(4-iodophenyl)porphyrinatomanganese(III) tetracyanoethenide, [MnTIPP][TCNE], **1I**, have been prepared and characterized as both the toluene and dichloromethane disolvates and the magnetic, IR, and thermal properties of these solvates, as well as their corresponding desolvated materials, have been determined and are compared to the previously reported $[TCNE]^{\bullet -}$ salts of 5,10,15,20-tetrakis(4-chlorophenyl)porphyrinatomanganese(III), **1Cl**. The ν_{CN} absorptions of **1X·2PhMe** (X = Cl, Br, I) and **1I·*x*CH_2Cl_2** occur at 2202 ± 1 (m) and 2161 ± 1 (s) cm^{-1} and **1X·*x*CH_2Cl_2** (X = F, Cl, Br) and **1F·*x*PhMe** occur at 2195 ± 1 (m) and 2135 ± 2 (s) cm^{-1}. Upon thermolysis at 175 °C the toluene desolvates to form α-[MnTXPP][TCNE] [X = Cl (α-**1C1**), Br (α-**1Br**), I (α-**1I**)] with ν_{CN} absorptions maintained at 2201 ± 1 (m) and 2160 ± 1 (s) cm^{-1}. In contrast, unlike **1Cl·2PhMe**, desolvation of **1X·2PhMe** (X = Br, I) in refluxing *n*-octane (127 °C) or heated mineral oil (170 °C) slurries does not lead to materials with ν_{CN} absorptions characteristic of β-[MnTClPP][TCNE]. Upon facile desolvation of dichloromethane solvates, materials with ν_{CN} absorptions characteristic of γ-[MnTClPP][TCNE] form as the ν_{CN} absorptions remain essentially unchanged [2195 ± 2 (m) and 2135 ± 2 (s) cm^{-1}]. The magnetic data for the [MnTXPP][TCNE] family are consistent with linear chain ferrimagnets comprised of antiferromagnetically coupled $S = 2$ Mn^{III} sites and $S = 1/2$ $[TCNE]^{\bullet -}$ sites with the antiferromagnetic intrachain coupling, J_{intra}/k_B (k_B = Boltzmann's constant) determined from fits to the Seiden expression for isolated chains comprised of alternating $S = 1/2$ and $S = 2$ spins. For the [MnTFPP][TCNE] series, J_{intra} values of −225, −160, −210, and −177 K were obtained for **1F·*x*PhMe**, β-**1F**, **1F·2CH_2Cl_2**, and γ-**1F**, respectively. While J_{intra} values of −30, −45, −270, and −75 K were observed for **1Br·2PhMe**, α-**1Br**, **1Br·2CH_2Cl_2**, and γ-**1Br**, respectively. Finally, J_{intra} values of −53, −35, −35, and −53 K were observed for **1I·2PhMe**, α-**1I**, **1I·2CH_2Cl_2**, and γ-**1I**, respectively. The ordering temperatures, T_c, determined from the maxima in the 10 Hz $\chi'(T)$ ranged from 6.5 K (**1I·2PhMe**) to 28 K for (**1F·*x*PhMe**). Based on the magnetic behavior, desolvation of **1X·PhMe** and **1X·CH_2Cl_2** increases the magnetic disorder and subsequent spin glass behavior as well as changing the observed interchain magnetic coupling.

Introduction

Over the past few years, the area of organic-based magnets has garnered considerable interest due to its potential technological importance[1] and multidisciplinary appeal.[2,3] This area of materials chemistry benefits from the rational design in preparing materials with predictable magnetic properties. There are a few basic approaches[3d,4] to designing magnetically ordered systems. One approach is to build systems in which dominant ferromagnetic magnetic coupling leads to a ferromagnet. A second approach is to antiferromagnetically couple spins of unequal magnitude leading to a net moment in the system, *i.e.*, ferrimagnetism. A number of ferrimagnetic 1-D heterometallic chain systems have been studied that exhibit bulk magnetic order.[3b,g,j,k,5,6] Examples of this approach include the ferrimagnet [Mn(NIT(*n*-Pr))(hfac)$_2$] [NIT(*n*-Pr) = 2-propyl-4,4,5,5-tetramethyl-4,5-dihydro-1*H*-imidazolyl-3-oxide-1-oxy; Hhfac = hexafluoroacetylacetonate] consisting of 1-D chains of Mn^{II} bridged by an $S = 1/2$ nitronyl nitroxide radical, and has T_c of 8.6 K.[3g,6a] More recently, through the use of polynitroxide ligands layered Mn(II) materials have been prepared with a T_c as high as 46 K.[6b] Herein, the work focuses on a system that contains the tetracyanoethylene radical anion, $[TCNE]^{\bullet -}$, that couples to spin-containing transition metal centers as typified by [MnTPP][TCNE]·2PhMe (H_2TPP = 5,10,15,20-tetraphenylporphyrin), which has a T_c of 15 K.[3b,7,8]

This metalloporphyrin family of electron transfer salts is especially interesting owing to its rich magnetic behavior.[3b,9] These 1-D chain structures are comprised of manganoporphyrins bridged by organic radicals such as $[TCNE]^{-}$,[9a] chloranil,[9d] or hexacyanobutadienide.[10] In the last few years, several substituted [MnTPP][TCNE] systems have been structurally and/or magnetically characterized.[8,9,11] Current research in this area focuses on the establishment of relationships between 3-D molecular structure and observed physical properties for this family of compounds.[12]

5,10,15,20-Tetraphenylmetalloporphyrins are appealing as model compounds due to the relative ease by which subtle changes in the porphyrin structure can be effected. Similarly, metalloporphyrins can accommodate a wide range of solvents[13] changing the intra- and inter-chain couplings and ultimately the T_c.[9e] As part of these studies the effects of

† Based on the presentation given at Dalton Discussion No. 3, 9–11th September 2000, University of Bologna, Italy.

Electronic supplementary information (ESI) available: rotatable 3-D crystal structure diagram in CHIME format. See http://www.rsc.org/suppdata/dt/b0/b003458o/

Table 1 Infrared ν_{CN} (cm^{-1}) stretching data for [MnTXPP][TCNE]·*x*solv (X = F, Cl, Br, I; solv = PhMe, CH_2Cl_2) and subsequent annealing products

	PhMe[b]	α[b]	β[b]	CH_2Cl_2[b]	γ[b]
	m s	m s	m s	m s	m s
	2195, 2133	2195, 2137		2196, 2136	2196, 2136
1F	***A***	***A***	[a]	***A***	***A***
	2201, 2160	2202, 2161	2190, 2132 ***A***	2195, 2138	2193, 2133
1Cl[9e]	***B***	***B***		***A***	***A***
	2203, 2162	2201, 2160	[a]	2195, 2137	2195, 2137
1Br	***B***	***B***		***A***	***A***
	2203, 2162	2201, 2160	[a]	2202, 2162	2202, 2162
1I	***B***	***B***		***B***	***B***

[a] Same as α-phase. [b] Type ***A*** or ***B*** as noted in the text.

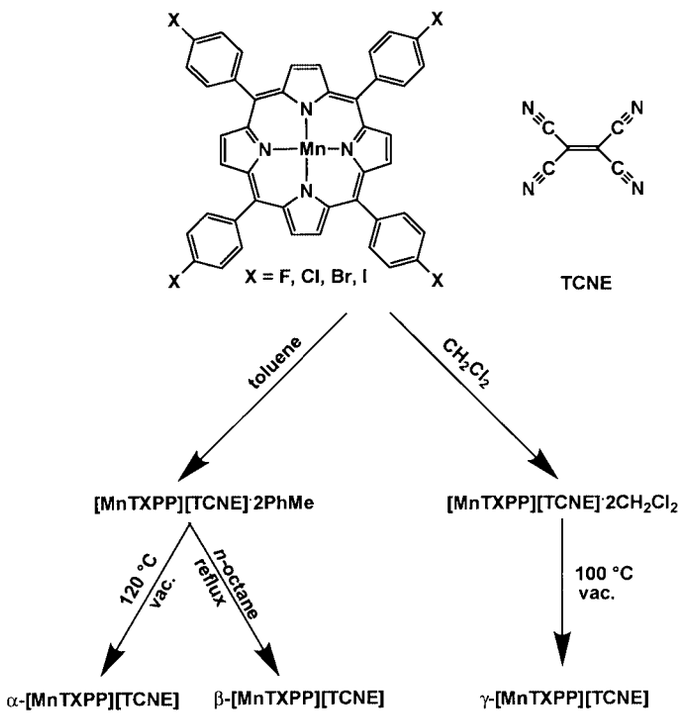

Scheme 1

thermal annealing on the toluene and dichloromethane solvates of *meso*-tetrakis(4-chlorophenyl)porphyrinatomanganese(III) tetracyanoethenide, [MnTClPP][TCNE], have been reported.[9e] The solvated and annealed desolvated products were prepared as illustrated in Scheme 1, with each of the five materials exhibiting distinctly different magnetic behavior. With the ultimate goal of preparing [MnTPP][TCNE] magnets with predictable and tunable physical properties, model systems that can be studied systematically to identify which structural parameters lead to observed ferrimagnetic 3-D magnetic ordering are sought. Recently we reported on a series of similarly structured 5,10,15,20-tetrakis(4-halogenophenyl)porphyrinatomanganese(II) electron transfer salts with TCNE prepared from toluene.[14] Within this series ordering temperatures as high as 28 K were observed. This doubling of T_c prompted us to revisit the influence of polymorphism and pseudopolymorphism in this class of compounds. As an extension of this earlier work, herein we report the structure of 5,10,15,20-tetrakis(4-bromophenyl)porphyrinatomanganese(III) tetracyanoethenide, [MnTBrPP][TCNE]· $2CH_2Cl_2$ (**1Br·2CH$_2$Cl$_2$**) as well as the thermal behavior and magnetic properties of the toluene and dichloromethane solvates of 5,10,15,20-tetrakis(4-fluorophenyl)porphyrinatomanganese(III) tetracyanoethenide, **1F**, 5,10,15,20-tetrakis(4-bromophenyl)porphyrinatomanganese(III) tetracyanoethenide, **1Br**, and 5,10,15,20-tetrakis(4-iodophenyl)porphyrinatomanganese(III) tetracyanoethenide, **1I** and compare these results to those observed for the 5,10,15,20-tetrakis(4-chlorophenyl)porphyrinatomanganese(III) tetracyanoethenide [MnTClPP][TCNE], **1Cl** family of magnets.

Results

Synthesis and thermal properties

The toluene and dichloromethane solvates of [MnTXPP][TCNE], (X = F, Cl,[9e] Br, I), **1X·*x*PhMe** and **1X·*x*CH$_2$Cl$_2$**, were prepared from the reaction of filtered solutions of Mn^{II}-TXPPpy and TCNE in toluene and dichloromethane, respectively. The presence of $[TCNE]^{\cdot -}$ was confirmed by the shift in the ν_{CN} absorption from neutral TCNE° [2259 (s), 2221 (m) cm^{-1}][7] to lower frequencies, which are summarized in Table 1. These values are similar to 2192 (s) and 2147 (m) cm^{-1} observed for [MnTPP][TCNE]·2PhMe[15] and 2197 (s) and 2133 (m) cm^{-1} for [MnTP′P][TCNE]·2PhMe [H_2TP′P = 5,10,15,20-tetrakis(3,5-di-*tert*-butyl-4-hydroxyphenyl)porphyrin];[9a] however, these data are inconsistent with the presence of $[TCNE]^{2-}$, [2104 (s), 2069 (m) cm^{-1}] or unbound $[TCNE]^{\cdot -}$, [2185 (s), 2145 (m) cm^{-1}].[4]

Except **1Cl·*x*CH$_2$Cl$_2$**, only a small shift in the ν_{CN} absorptions were observed upon thermal treatment under reduced pressure of the toluene solvates (Table 1) indicating little change in the $[TCNE]^{\cdot -}$ bonding and consequently the intrachain structure

Table 2 Summary of structural parameters for[MnTXPP][TCNE]·*x*solv

Compound	Mn · · · Mn Intrachain/Å	Mn · · · Mn Interchain/Å	Intrachain · · · Intrachain/Å	Interchain separations/Å	Mn–N–C/°	MnN_4–TCNE dihedral angle, δ/°
1Cl·2PhMe[9e]	10.189	10.171	2.267	8.858	167.2	86.8
		11.458		13.850		
		14.522		16.474		
1Br·2PhMe[14]	10.277	10.079	2.293	9.409	168.1	89.4
		11.530		14.001		
		14.626		16.830		
1I·2PhMe[14]	10.101	9.831	2.276	9.390	158.7	69.6
		11.823		15.213		
		15.399		16.703		
1Cl·2CH_2Cl_2[9e]	9.894	10.697	2.276	10.697	143.1	52.4
		12.958		12.727		
1Br·2CH_2Cl_2	9.973	10.823	2.290	10.823	145.0	52.9
		13.127		12.798		
1H·2PhMe[7a]	10.116	11.006	2.306	10.201	147.6	55.4
		11.829		13.139		
		13.269		13.630		

occurs. The subsequent desolvated materials were designated as α-, β- or γ-phases in accord with the designation of the original chloro-substituted series and method of preparation, Scheme 1. In general the TGA/MS of **1X·*x*PhMe** indicate two weight losses; the first ranging from 98 to 197 °C and the second at 300 °C. The low temperature weight loss is accompanied by the appearance of toluene (m/z^+ 91) in the mass spectrum and predicts 1.19, 2.2, and 1.8 toluene solvates per formula unit for X = F, Br, and I, respectively. The high temperature weight loss (above 300 °C) is due to TCNE decomposition, based on the appearance of characteristic TCNE fragments in the mass spectrum. Interestingly, **1F·*x*PhMe** has one toluene compared with **1Cl·2PhMe**, **1Br·2PhMe**, and **1I·2PhMe** which accommodates two toluenes per formula unit, possibly due to contraction of the crystal lattice or close interchain spacing for the former. The temperature of solvent loss for **1F·*x*PhMe** is significantly higher, 197 °C, than observed for other halogens, again consistent with a more tightly held solvent.

For X = Br and I, samples heated above 120 °C under vacuum in excess of 2 h showed no evidence of toluene in the TGA/MS, with α-**1X** collected 30 min after complete desolvation. Thermolysis of **1Br·2PhMe**, in *n*-octane at (127 °C) leads to the isolation of β-**1Br**, akin to β-**1Cl**, but had ν_{CN} absorptions characteristic of α-**1Br** over the measurable temperature range (−134 to 180 °C). Heating **1Br·2PhMe** in mineral oil to 170 °C (well below the decomposition temperature) for periods up to 16 h did not result in a noticeable change in the ν_{CN} absorptions. Heating in excess of 16 h was accompanied by signs of decomposition, suggesting that the thermal formation β-**1Br** is not possible by this methodology. Unlike **1Cl·2PhMe** that exhibits weight loss above 78 °C, **1Br·2PhMe** requires significantly higher temperatures (97 °C) for desolvation.

Thermal desolvation of **1I·2PhMe** in *n*-octane at 127 °C was accompanied by a negligible shift in ν_{CN} to 2201 (s) and 2160 (m) cm^{-1}. Formation of α-**1I** was monitored by TGA/MS with complete desolvation observed in 2 h and the subsequent α-phase, α-**1I**, isolated 30 min thereafter. Thermolysis at 170 °C in mineral oil leads to a product whose ν_{CN} absorptions are again identical to α-**1I** over the measurable temperature range (−134 to 180 °C). Again attempts to prepare β-**1I** by heating to temperatures in excess of 200 °C for extended periods led to decomposition.

Due to rapid solvent loss, detailed thermo-physical measurements for **1X·2CH_2Cl_2** (X = F, Cl, Br, I) were not possible; however, detailed magnetic experiments were performed on solvated materials with the use of an airtight sample holder. As with **1Cl·2CH_2Cl_2**,[9e] complete desolvation of **1X·2CH_2Cl_2** (X = F, Br, I) to form γ-**1X** did not alter the ν_{CN} absorptions. As the ν_{CN} absorptions are sensitive to changes in the local coordination environment around Mn, the desolvation of **1X·2CH_2Cl_2** is assumed to proceed with minimal changes in the intrachain structure. Hence, desolvation likely effects the magnitude of interchain coupling interactions and ultimately the 3-D magnetic ordering temperatures, T_c. In the related 1-D heterometallic chain $[CoCu(pbaOH)(H_2O)_x]$ ($x < 3$)[5b] [pbaOH = 2-hydroxy-1,2-propanediylbis(oxamato)] for example, the removal of successive water molecules caused the ordering temperature to increase from <2, 10, 38 K for $x = 3$, 2, and 1, respectively. This is attributed to an increase in both structural and magnetic dimensionality.[5b] In the present system, desolvation should decrease the interchain spacing, and assuming the 1-D stacking remains constant, stronger interchain coupling and higher ordering temperatures are expected (*vide supra*).

Structure

The detailed structures of **1X·2PhMe** (X = Cl, Br, I) were previously described.[9e,14] The solid state motifs of **1X·2PhMe** (X = Cl, Br, I) are comprised of similar 1-D chains of · · · $D^+A^-D^+A^-$ · · · where the $[TCNE]^{\bullet -}$ is *trans*-μ-*N*-σ-bound to two $[Mn^{III}TXPP]^+$ cations, which stack along the crystallographic *b* axis. Along *a* the chains interdigitate with the phenyl groups on each adjacent chain pointing between the porphyrin planes of the closest chain to form 2-D layers parallel to *a*. Close contacts were observed between the halogen X(1) and C(1) of $[TCNE]^{\bullet -}$ of 3.371, 3.481, and 3.848 Å for **1Cl·2PhMe**,[9e] **1Br·2PhMe**,[14] and **1I·2PhMe**,[14] respectively. The resulting 2-D layers stack along *c* separated by columns of solvent. The structural details for the toluene and the dichloromethane solvates are summarized in Table 2.

The structure determination of **1Br·2CH_2Cl_2** revealed one-half of an ordered **1Br·2CH_2Cl_2** with both the cation and anion occupying special positions in the unit cell, Fig. 1. The $Mn–N_{ring}$ bond distances are 2.009(2) and 2.014(2) Å for **1Cl·2CH_2Cl_2**[16] and 2.010(7) and 2.004(7) Å for **1Br·2CH_2Cl_2** with the remaining bond distances and angles typical of $[Mn^{III}TPP]^+$.[9,10,12,17] As with the majority of $[TCNE]^{\bullet -}$ coordination polymer structures, $[TCNE]^{\bullet -}$ is planar with a twist of 0.0°. The $[TCNE]^{\bullet -}$ bond distances for **1Br·2CH_2Cl_2** are consistent with other know $[TCNE]^{\bullet -}$ structures, with the key central C–C distance being 1.43(2) Å.[14] The Mn^{III} in **1Br·2CH_2Cl_2** occupies a tetragonally elongated octahedral coordination sphere with a Mn–NC bond distance of 2.290(6) Å, which is identical to [MnTOMePP][TCNE]·2PhMe (2.290 Å) [H_2TOMePP = 5,10,15,20-tetrakis(4-methoxyphenyl)porphyrin],[9d] and within experimental error of [MnTPP][TCNE] (2.306 Å),[9a] and **1Br·2CH_2Cl_2** (2.276 Å), but is significantly shorter than that of the [MnOEP][TCNE],[10]

(H_2OEP = octaethylporphyrin) (2.361 Å). The solid state motif of **1X·2CH$_2$Cl$_2$** (X = Cl and Br) are comprised of nearly isostructural 1-D coordination polymers of alternating $\cdots D^+A^-D^+A^-\cdots$ where the $[TCNE]^{\cdot -}$ (A) is *trans*-μ-*N*-σ-bound to $[MnTXPP]^+$ (D) cations. The Mn–N–C angles of **1X·2CH$_2$Cl$_2$** (X = Cl, Br) are 143.1 and 145.0°, respectively, with the dihedral angles between the mean planes of porphyrin MnN_4 and $[TCNE]^{\cdot -}$ of 52.4[9e] and 52.9°. Intrachain Mn···Mn separations of 9.8949[e] and 9.973 Å for **1X·2CH$_2$Cl$_2$** (X = Cl and Br) respectively, fall in the typical range for [Mn(porphyrin)][TCNE] chains.[9] The interchain distances for **1Br·2CH$_2$Cl$_2$** are depicted in Fig. 2 and summarized in Table 2. While each member of the [Mn(porphyrin)][TCNE] family[5–9] is comprised of parallel 1-D $\cdots D^+A^{\cdot -}D^+A^{\cdot -}\cdots$ chains, the intrachain arrangement of **1X·2CH$_2$Cl$_2$** (X = Cl, Br) is unusual with respect to the other family members, both form a herringbone arrangement between adjacent chains, Fig. 2. Similar packing was observed in $[MnTF_4OMePP][TCNE]\cdot 2PhMe$[18] [$H_2TF_4$-OMePP = 5,10,15,20-tetrakis(2,3,5,6-tetrafluoro-4-methoxyphenyl)porphyrin], which also crystallizes in the $P2_1/n$ space group at higher temperatures. The chains interdigitate along *b* to form layers with the halogen of adjacent chains pointed into the gap between the $[TCNE]^{\cdot -}$ bridged porphyrins as observed in the toluene solvates.[14] Close contacts were observed between the *para*-halogen and $[TCNE]^{\cdot -}$ of 3.401 and 3.490 Å for **1Cl·2CH$_2$Cl$_2$** and **1Br·2CH$_2$Cl$_2$**, respectively. This observation is consistent with the toluene series **1X·2PhMe** (X = Cl, Br, I), which exhibit similar *para*-halogen–$[TCNE]^{\cdot -}$ contacts (*vide infra*). Although the genesis of this interaction is not well understood, similar halogen–$[TCNE]^{\cdot -}$ contacts have been observed in $[MnTF_4OMePP][TCNE]\cdot 2PhMe$ and $[MnT(o\text{-}F)PP][TCNE]\cdot 2PhMe$[18] and many play a role in the chain orientation.[9f]

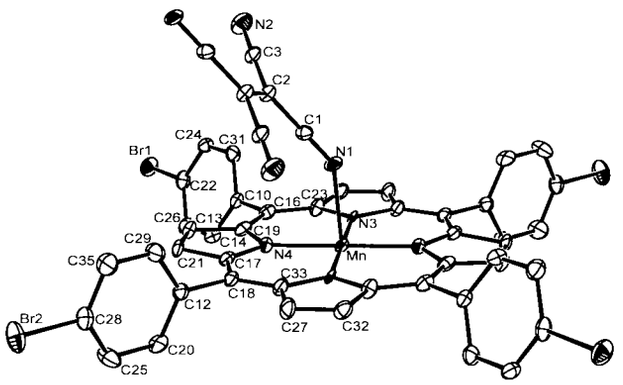

Fig. 1 Labeling diagram and ORTEP[30] (30% probability level) diagram for $[MnTBrPP][TCNE]\cdot 2CH_2Cl_2$, **1Br·2CH$_2Cl_2$**.

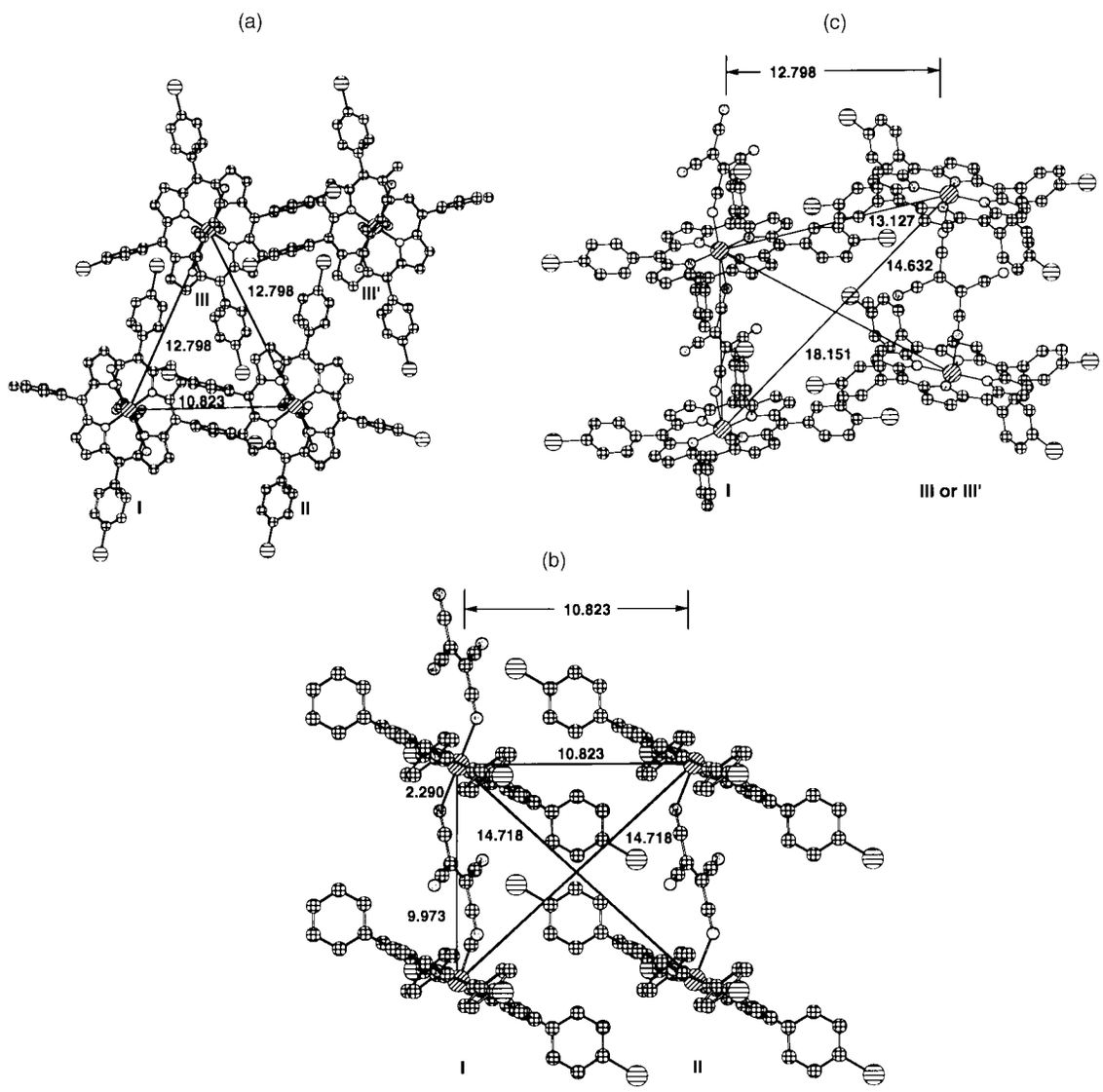

Fig. 2 View down the crystallographic *b* (chain) axis (a) and parallel to *b* showing the intra- and inter-chain interaction among the unique chains: **I**–**II** (b), and **I**–**III** (=**I**–**III**′) (c) for $[MnTBrPP][TCNE]\cdot 2CH_2Cl_2$, **1Br·2CH$_2Cl_2$**. Note the $[TCNE]^{\cdot -}$ *trans*-μ-*N*-σ-bonding to $[MnTClPP]^+$ and the uniform chains. The hydrogen atoms and toluenes of solvation are omitted for clarity.

Table 3 Summary of magnetic properties for [MnTPP][TCNE]·*x*solv

Complex, type	μ_{eff}/μ_B	θ/K	θ'/K	T_{min}/K	J_{intra}/k_B/K		T_c[c]/K	φ	M(5 T, 2 K)/ Kemu Oe mol^{-1}
					a	*b*			
1F·*x*PhMe,[14] ***A***	5.12	[d]	70	667[c]	−225	−159	28.0	0.005	12.3
α-**1F**, ***A***	5.10	[d]	64	474[e]	−160	−113	24.5	0.02	11.5
1F·2CH$_2$Cl$_2$, ***A***	5.19	[d]	55	609[c]	−210	−145	26.9	0.012	10.5
γ-**1F**, ***A***	5.19	[d]	38	520[e]	−177	−124	25.4	0.013	12.7
1Cl·2PhMe,[9e] ***B***	4.69	−60	13	110	−33	−26	8.8	0.017	11.0
α-**1Cl**,[9e] ***B***	4.89	−10	29	192	−65	−46	6.7	0.15	18.5
β-**1Cl**,[9e] ***A***	5.05	[d]	92	800[e]	−267	−190	11.1	0.14	15.8
1Cl·2CH$_2$Cl$_2$,[9e] ***A***	5.10	[d]	58	480[e]	−160	−114	14.1	0.001	14.0
γ-**1Cl**,[9e] ***A***	5.40	[d]	86	793[e]	−265	−189	10.8	0.1	18.7
1Br·2PhMe,[14] ***B***	5.44	−53	13	80	−30	−19	8.0	0.005	12.5
α-**1Br**, ***B***	4.88	−37	17	122	−45	−29	6.5	0.057	19.5
1Br·2CH$_2$Cl$_2$, ***A***	5.17	[d]	97	790[e]	−270	−188	10.0	0.10	13.3
γ-**1Br**, ***A***	5.60	−30	40	220	−75	−52	10.5	0.12	14.5
1I·2PhMe,[14] ***B***	5.08	−79	30	160	−53	−38	6.5	0.17	11.0
α-**1I**, ***B***	5.19	−118	15	105	−35	−25	4.9	0.14	11.1
1I·2CH$_2$Cl$_2$, ***B***	5.50	−104	15	110	−35	−26	6.6	0.13	11.5
γ-**1I**, ***B***	5.24	−156	24	141	−53	−34	7.6	0.11	10.1
1H·2PhMe[7]	5.12	[d]	61	270	−115	−64	13.0	0.18	17.5

[a] J_{intra} was obtained from the Seiden expression. [b] $J_{intra} = T_{min}/4.2$, see text. [c] Maximum in $\chi'(T, 10\ Hz)$. [d] Not observed. [e] From fit to Seiden model. [f] emu Oe mol^{-1} = 10^2 A mmol^{-1}.

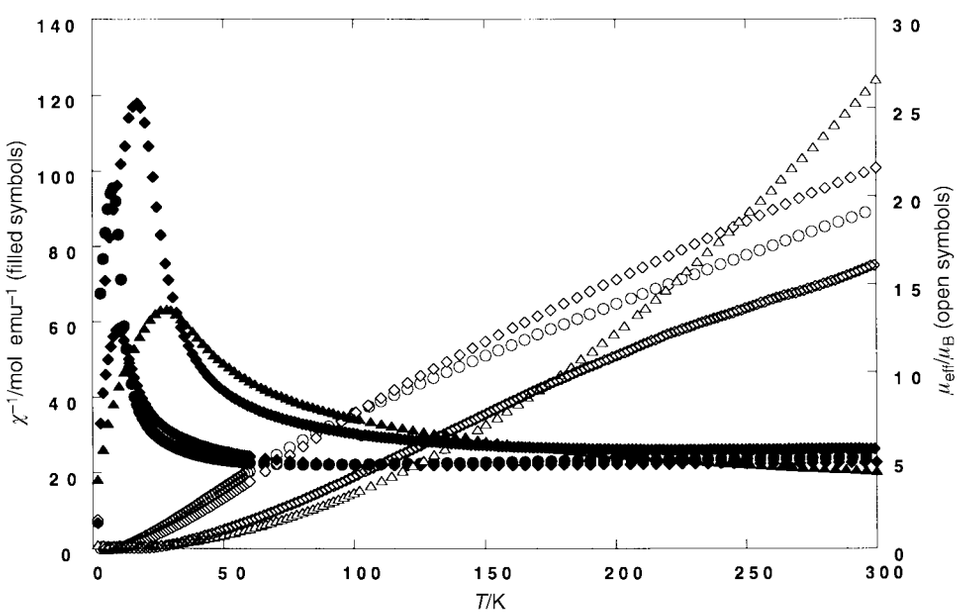

Fig. 3 Reciprocal molar magnetic susceptibility, χ^{-1} (filled symbols), and moment, μ_{eff} (open symbols), as a function of temperature (1000 Oe) for (a) **Br·2PhMe** (o, ●), (b) α-**1Br** (□, ■), (c) **1Br·2CH$_2$Cl$_2$** (△, ▲), and (d) γ-**1Br** (◇, ◆).

Magnetic studies

The magnetic behavior of [MnTXPP][TCNE]·solv (X = F, Cl, Br, I; solv = PhMe, CH_2Cl_2) are similar, and the bromo-series was chosen as a model and the F and I series are discussed and summarized in Table 3. The 2 to 300 K reciprocal susceptibility, χ^{-1}, and effective moment, μ_{eff}, of **1Br·2PhMe**, α-**1Br**, **1Br·2CH$_2$Cl$_2$**, and γ-**1Br** are shown in Fig. 3. The 300 K effective moments range from 4.88 to 5.60 μ_B averaging 5.26 μ_B, close to the expectation for noninteracting $S = 2$ and $S = 1/2$ spins. Values less that 5.20 μ_B are due to antiferromagnetic coupling evident at room temperature, while values higher than 5.20 μ_B are likely due to errors in molecular weight due to the specific degree of solvation, or conversely a consequence of interchain coupling, strong coupling with $T_{min} \gg 300$ K.[18]

The susceptibilities of **1Br·2PhMe** and α-**1Br** can be fit to a Curie–Weiss expression, χ [$\propto 1/(T - \theta)$] in two linear regions. The linear high temperature regime above 150 K can be fit with θ values of −53 and −37 K for **1Br·2PhMe** and α-**1Br**, respectively indicative of dominant antiferromagnetic coupling. Between 20 and 100 K the data can be fit with effective θ,[9] θ', of 13 K for **1Br·2PhMe** and 17 K α-**1Br**, indicative of long range ferromagnetic coupling. Upon desolvation of **1Br·2PhMe** θ and θ' values of −37 and 17 K were observed. The 30% increase in θ' with desolvation in **1Br·2PhMe** is less than the 123% increase observed in **1Cl·2PhMe**; however, both suggest the magnitude of the interchain coupling is increased upon desolvation possibly due to a contraction of interlayer spacing. **1Br·2CH$_2$Cl$_2$** exhibits a single linear regime in $\chi^{-1}(T)$ above a temperature of 50 K that was fit with an θ' value of 97 K, the highest reported θ value for the [MnTPP][TCNE] family, significantly higher than that of [MnTPP][TCNE]·2PhMe[7] 61 K and close to that of β-**1Cl** 92 K.[9e] Desolvation of **1Br·2CH$_2$Cl$_2$** yields γ-**1Br**, which is accompanied with a 41% decrease in θ' (40 K) and the observation of θ of −30 K. This is in stark contrast to **1Cl·2CH$_2$Cl$_2$** which exhibits a 48% increase in θ' upon desolvation. Hence, the operative mechanisms of desolvation of **1Cl·2CH$_2$Cl$_2$** and **1Br·2CH$_2$Cl$_2$** are likely different, which is surprising given their structural similarities. The $\chi T(T)$ of **1Br·2PhMe**, α-**1Br** and γ-**1Br** are characterized by

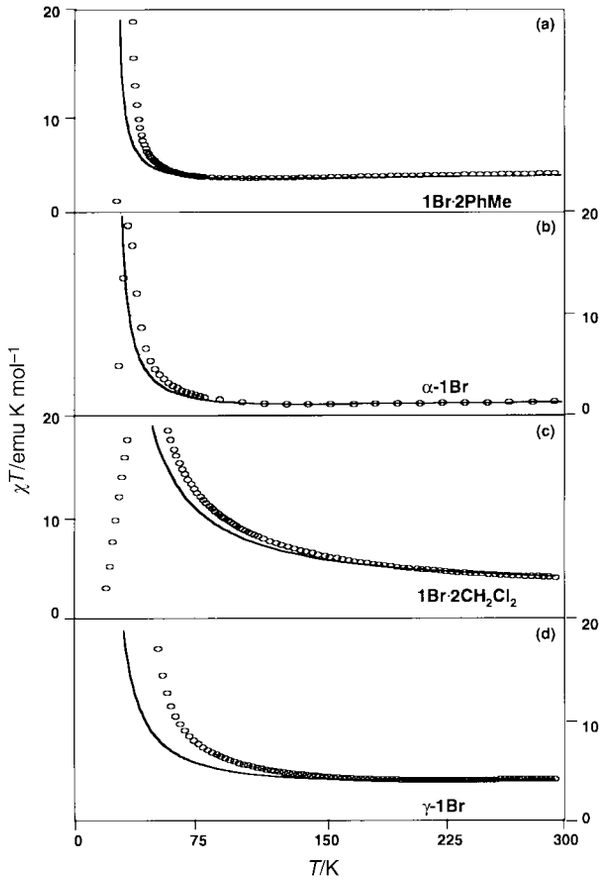

Fig. 4 Fit of the $\chi T(T)$ data to the Seiden expression[19] for (a) **1Br·2PhMe**, (b) α-**1Br**, (c) **1Br·2CH$_2$Cl$_2$**, and (d) γ-**1Br**.

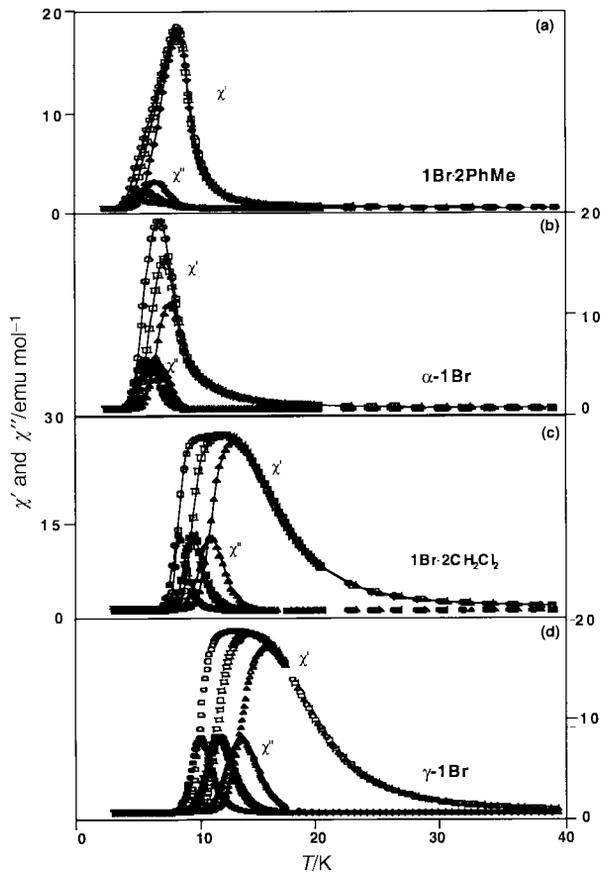

Fig. 5 Temperature dependencies of the dispersive, χ' (⊖, ■, and ⊖) and absorptive, χ'' (×, ■, and ○), components of the ac susceptibility at 10, 10^2, and 10^3 Hz, respectively, (a) **1Br·2PhMe**, (b) α-**1Br**, (c) **1Br·2CH$_2$Cl$_2$**, and (d) γ-**1Br**. (H_{dc} = 0 Oe, amplitude = 1 Oe.) Samples were zero-field cooled and data taken upon warming.

a decrease in $\chi T(T)$ with decreasing temperature reaching a minimum at 80, 122, and 220 K for **1Br·2PhMe**, α-**1Br** and γ-**1Br**, respectively. Similar results are observed for **1F** and **1I**, Table 3.

The 1-D antiferromagnetic intrachain coupling, J_{intra}, of the [MnTBrPP][TCNE] series was determined from modeling $\chi T(T)$ to the Seiden[19] expression, $H = -2J_{intra}\boldsymbol{S}_a\cdot\boldsymbol{S}_b$ with J_{intra}/k_B values of −30,[14] −45, −270, and −75 K for **1Br·2PhMe**, β-**1Br**, **1Br·2CH$_2$Cl$_2$**, and γ-**1Br** respectively, Table 3 and Fig. 4. The T_{min} of 790 K was estimated from the Seiden model for **1Br·2CH$_2$Cl$_2$**. Reasonable fits were not obtained for **1Br·2PhMe** or γ-**1Br**, however, the shape and position of the minimum in $\chi T(T)$ was modeled to estimate J_{intra} from the Seiden expression.[19] The Seiden model may not be valid for systems for which the intrachain coupling is weak, likely due to next nearest neighbor interactions. Alternatively, J_{intra} can be estimated from the expression $J_{intra}/k_B = T_{min}/4.2$[20] yielding values of −19, −29, −188 and −52 K for **1Br·2PhMe**, β-**1Br**, **1Br·2CH$_2$Cl$_2$**, and γ-**1Br**, respectively. The coupling of $[TCNE]^{\cdot-}$ with Mn^{III} is predicted to be antiferromagnetic, $J_{intra} < 0$, based on orbital overlap considerations.[21] An inverse correlation between θ' and the dihedral angle between the porphyrin MnN_4 and $[TCNE]^{\cdot-}$ mean planes as well as the Mn–N–C bond angle has been established.[22] Although no structural data are available for the desolvated materials, using the correlation between θ' or T_{min} and dihedral angle, δ, between the $[TCNE]^{\cdot-}$ and the porphyrin MnN_4 mean planes, estimates of the dihedral angles of the desolvated materials, Table 2, can be made. Based on this linear correlation, we predict dihedral angles of 86, 82, 44, and 73° for **1Br·2PhMe**, β-**1Br**, **1Br·2CH$_2$Cl$_2$**, and γ-**1Br**, respectively.

Ordering temperatures for **1Br·2PhMe**, β-**1Br**, **1Br·2CH$_2$Cl$_2$**, and γ-**1Br** were determined by the initial peak in the in-phase susceptibility at 10 Hz, $\chi'(T)$, and are 8.0, 6.5, 10.0, and 10.5 K, respectively (Fig. 5). The initial peak in $\chi'(T)$ for **1Br·2PhMe** was not accompanied by a peak in $\chi''(T)$ suggesting an antiferromagnetic, not a ferrimagnetic state. As the temperature is decreased a second peak in $\chi'(T)$ is observed as a shoulder of the first peak, which shows frequency dependence as well as $\chi''(T)$ component, suggesting that a spin-glass or disordered state is entered. This reentrant behavior was previously observed for [MnTPP][TCNE]·2PhMe.[9a] Frequency dependence observed in these materials can be parameterized $\{\varphi = \Delta T_f/T_f\log\Delta\omega\}$[23] ($T_f = T$ at which $\chi'(T)$ has a maximum at the lowest frequency measured; ΔT_f = difference $\chi'(T)$ as a maxima at the lowest and highest frequencies measured; ω = frequency) and yield values ranging from $\varphi = 0.005$ to 0.17 consistent with typical spin-glasses, *e.g.*, the alloys of *Pd*Mn $\varphi = 0.013$ and *Ni*Mn $\varphi = 0.018$.[23] The observation of a crystallographic phase transition in the related [MnTF$_4$OMePP][TCNE]·2PhMe[18] suggests disorder at low temperatures may be due to incomplete crystallographic phase changes near the magnetic ordering temperature. α-**1Br** is characterized by a single frequency dependent peak in $\chi'(T)$ and $\chi''(T)$ at 6.5 K and 5.3 K, respectively. The position of the initial peak in $\chi'(T)$ is coincident with the shoulder observed in **1Br·2PhMe** and is likely due to partial desolvation of **1Br·2PhMe** during sample preparation. Desolvation of **1Br·2PhMe** leads to a 19% decrease in the ordering temperature similar to **1F·*x*PhMe** (13%) and **1Cl·2PhMe** (24%). Likewise, desolvation of **1X·2CH$_2$Cl$_2$** leads to a decrease in T_c of 5.6% (F) for 23% (Cl), and interestingly an increase in T_c of 5.0% (Br) for 15% (I) (Table 3).

Isothermal magnetization data were collected in the zero-field cooled (ZFC) state at several temperatures. The 2 K, at 5 T magnetization of the [MnTBrPP][TCNE] family are summarized in Table 3 and range from 12 500 to 19 500 emu Oe mol^{-1}

Table 4 Crystallographic data for [MnTBrPP][TCNE]·2CH_2Cl_2

	[MnTBrPP][TCNE]·2CH_2Cl_2
Formula	$C_{52}H_{28}N_8MnBr_4Cl_4$
M	1281.24
Space group	$P2_1/n$
a/Å	9.973(5)
b/Å	10.824(5)
c/Å	23.584(15)
β/°	100.24(6)
Z	2
V/Å^3	2505.32
Reflections collected	4930
Independent reflections	4389
λ (MoK_α)/Å	0.71073
$R(F_o)$	0.0589
$Rw(F_o)$	0.0691
μ/mm^{-1}	0.344
T/K	225

averaging 14 950 emu Oe mol^{-1}. Saturation below 5 T was not observed possibly due to spin canting; however, at significantly higher fields M should approach the expectation of 16 755 emu Oe mol^{-1} for an isolated antiferromagnetic ($S_{tot} = 2 - 1/2$) system, but this has yet to be achieved for any members of this family of magnets even in field as high as 120 000 Oe.[24]

Magnetic-like behavior below 10 K is also observed for the [MnTXPP][TCNE] family with critical fields ranging from 4.0 to 27.0 kOe as well as large coercive fields and remanent magnetizations at low temperature. These interesting temperature dependent behaviors are present for the entire family of manganoporphyrin–TCNE magnets and is discussed independently.[18]

Discussion

Some trends emerge from the thermal studies of the [MnTXPP][TCNE] series of compounds. For X = F the ν_{CN} absorptions are invariant to solvent or thermal history, with absorptions of 2195.5 ± 1 (m) and 2135 ± 2 (s) cm^{-1}, which based on ν_{CN} are assigned to a type ***A*** material. Likewise, for X = I only ν_{CN} absorptions of 2201 ± 1 (m) and 2161 ± 1 (s) cm^{-1} were observed, which are assigned to type ***B*** material. In this context, type ***A*** and ***B*** refer to materials with the lower frequency ν_{CN} absorption assigned to ν_{MeCN} being ≈2135 or ≈2160 cm^{-1}. **1Cl·2PhMe** is unique in exhibiting two thermally isolated phases from the toluene solvate belonging to both type ***B*** (α-**1Cl**) and ***A*** (β-**1Cl**).[9e] The dichloromethane solvate **1X·*x*CH_2Cl_2** and subsequent desolvated phases, γ-**1X**, (X = F, Cl, Br) are type ***A*** materials. Surprisingly, **1I·*x*CH_2Cl_2** and γ-**1I** belong to type ***B***. Prolonged heating at elevated temperatures of **1X·2PhMe** (X = Br, I) does not yield β-**1X** (X = Br, I) below the decomposition temperature. Therefore, transformation from type ***B*** to type ***A*** was only observed in **1Cl·2PhMe**. The frequency ν_{CN} absorption is indicative of the coordination environment of the Mn^{III} center, with lower frequencies suggesting stronger back-bonding with [TCNE]$^{\cdot -}$. Hence, type ***A*** materials have less back-bonding than materials of type ***B***. These data suggest the steric size of the halogen may ultimately govern the intrachain stacking and hence the infrared absorptions observed for the *para*-halogen substituted [MnTPP][TCNE] series. Small halogens (X = F) tend to form type ***A*** materials with large halogens (X = Br, I) favoring type ***B*** materials, with X = Cl being borderline. Note that ***A*** and ***B*** refer to intrachain structures as the ν_{CN} data reflect local [TCNE]$^{\cdot -}$ bonding and hence do not reflect changes in the interchain interactions which govern the 3-D bulk magnetic behavior.

From the 1-D **1X·2PhMe** (X = Cl, Br, I) structures some conclusions can be reached as to the mechanism of β-**1Cl** formation and the absence of β-**1Br** or β-**1I**. Conversion of **1Cl·2PhMe** to β-**1Cl** is attributed to the collapse of the chain structure. Thus, in **1Cl·2PhMe** chlorine is small enough to allow the porphyrin planes to slide closer together to form a structure similar to **1Cl·2CH_2Cl_2**. Thermal annealing of **1X·2PhMe** (X = Br, I) does not lead to isolation of β-**1X** with prolonged heating eventually leading to decomposition. The increased size of the bromo- and iodo-substituent requires more steric space and thermal energy to collapse the intrachain stacking.

The study of the magnetic properties can be divided into two regimes: (i) the high temperature regime characterized by antiferromagnetic coupling of the [TCNE]$^{\cdot -}$ radical with the Mn^{III} center and (ii) the low temperature magnetic behavior characterized by observation of magnetic ordering. The magnetic behavior of the [MnTPP][TCNE] family of magnets is exceedingly complicated and not readily modeled over a large temperature range. To account for the onset of 3-D ordering we must approach the spin coupling from the simplest model. A simple nearest neighbor exchange interaction can be described by spin Hamiltonian, $H = -2J\boldsymbol{S}_1\cdot\boldsymbol{S}_2$, where $\boldsymbol{S}_1$ and $\boldsymbol{S}_2$ are neighboring spin sites and J represents the coupling between the two spins.[25] The sign and magnitude of the exchange parameter, J, depends largely upon the system studied. In [MnTXPP][TCNE], J is dominated by the 1-D antiferromagnetic coupling between Mn^{III} and [TCNE]$^{\cdot -}$. In the high temperature regime the magnetic data can, in most cases, can be modeled by the Seiden expression[19] for isolated chains of alternating quantum and classical $S = 2$ and quantum $S = 1/2$ spins and J_{intra}. In cases where the 1-D coupling is weak, the Seiden model does not adequately describe the coupling at high temperatures. Likely, the intrachain exchange would need to be expanded to include such effects as temperature independent paramagnetism, TIP, and single ion anisotropy.[26] Hence, as noted the analytical expression $T_{min}/4.2$ is used to estimate the 1-D coupling J_{intra} in those special cases.[20] At low temperatures typically T <30 K, 2- and 3-D interactions can no longer be neglected and the Seiden model is no longer valid.

Conclusion

The structural and magnetic properties have been described for a series of *para*-halogenated [MnTXPP][TCNE] derivatives prepared from toluene and from dichloromethane. The structure of the toluene solvates are found to form similar 1-D chains which form loosely knit layers separated by columns of solvent with all chains stacking parallel to the crystallographic b axis. The structurally characterized dichloromethane solvates also form similar 1-D chains that form layers through close contacts between chains with columns of solvent separating the layers. Effects of thermal annealing were studied for both solvates. It was found that the nature of the effects of annealing are system dependent with no clear relationship between the halogen series. Toluene solvates of larger halogens were found to exhibit increased thermal stability of the 1-D structure based on the ν_{CN} absorptions, which for **1Br·2PhMe** or **1I·2PhMe** were unchanged below the decomposition temperature.

The 1-D magnetic coupling for the majority of the systems studied was modeled by the Seiden function with J_{inter} values ranging from −30 to −270 K. The T_c's of the CH_2Cl_2 solvates exceed the T_c's for the related PhMe solvates for type ***B*** PhMe containing materials but for type ***A*** PhMe solvates the opposite is true. Although exceptions occur desolvation decreases T_c, except for the PhMe solvate for X = Cl, and the CH_2Cl_2 solvates for X = Br and I. Also as expected the disorder, as determined for the change in the maxima of $\chi'(T)$ as a function frequency, φ, increases upon thermal treatment with both solvates for X = I being an exception. These trends as well as their exceptions are the subject of further studies.

We are currently studying the complete halogen–porphyrin series as model systems to understand and ultimately control the supramolecular crystal packing. Furthermore, with the high critical temperatures observed for the [MnTFPP][TCNE] series, we are focusing on fluorinated porphyrins to identify which possible structural factors influence the ordering temperature for the series.

Experimental

Synthesis

All manipulations involving $[TCNE]^{\bullet -}$ were carried out under nitrogen using standard Schlenck techniques or in a Vacuum Atmospheres DriLab®. Pyridine (py) and solvents used for the preparation of the $[TCNE]^{\bullet -}$ salts were predried and distilled from appropriate drying agents. TCNE was obtained as a gift from O. Webster and was resublimed prior to use. Mn^{II}TXPPpy (X = F, Br, I) were prepared by literature methods. [Mn^{III}TClPP][TCNE]·2PhMe (**1Cl·2PhMe**), α-[Mn^{III}TClPP][TCNE] (α-**1Cl**), β-[Mn^{III}TClPP][TCNE] (β-**1Cl**), [Mn^{III}TClPP][TCNE]·$2CH_2Cl_2$, (**1Cl·2CH$_2$Cl$_2$**), γ-[Mn^{III}TClPP][TCNE], (γ-**1Cl**), [Mn^{III}TFPP][TCNE]·*x*PhMe, (**1F·*x*PhMe**), [Mn^{III}TBrPP][TCNE]·2PhMe (**1Br·2PhMe**), and [Mn^{III}TIPP][TCNE]·2PhMe, (**1I·2PhMe**) were prepared as previously reported.[9e,14] Unless noted, attempts to grow crystals suitable for single crystal X-ray diffraction studies failed.

α-[MnTFPP][TCNE] (α-1F). A glass vial containing freshly prepared [MnTFPP][TCNE]·*x*PhMe (*ca.* 30 mg) was heated in a tube furnace under dynamic vacuum at 175 °C for 3 h. Product formation was monitored by TGA/MS with heating continued ≈1 h after desolvation was achieved. IR (Nujol; cm^{-1}): ν_{CN} 2195 (m), 2137 (s). Calc. for [MnTFPP][TCNE] ($C_{50}H_{24}F_4MnN_8$) *M* 867.71; C, 69.21; H, 2.79; N, 12.91. Found C, 68.89; H, 3.01; N, 12.82%.

[MnTFPP][TCNE]·2CH$_2$Cl$_2$ (1F·2CH$_2$Cl$_2$). Filtered 10 mL CH_2Cl_2 solutions of Mn^{II}TFPPpy (16.0 mg, 0.0195 mmol) and TCNE (10 mg, 0.080 mmol) were mixed and stirred under nitrogen at room temperature for 4 h. The mixture was then layered with 40 mL of Et_2O and transferred to a −25 °C freezer where the reaction mixture was allowed to stand for 3 days in an inert atmosphere glovebox. The resulting dark green microcrystalline precipitate was collected by vacuum filtration. IR (Nujol; cm^{-1}): ν_{CN} 2196 (m), 2136 (s).

γ-[MnTFPP][TCNE] (γ-1F). The desolvated, γ-**1F·2CH$_2$Cl$_2$**, was obtained by drying [MnTFPP][TCNE]·$2CH_2Cl_2$ under reduced pressure for 1 h at room temperature, yielding 9.5 mg (86%) of dark green microcrystalline powder. IR (Nujol; cm^{-1}): ν_{CN} 2196 (m), 2136 (s). Calc. for [MnTFPP][TCNE] ($C_{50}H_{24}F_4MnN_8$) *M* 867.71. C, 69.21; H, 2.79; N, 12.91. Found C, 68.99; H, 2.84; N, 13.15%.

α-[MnTBrPP][TCNE] (α-1Br). α-**1Br·2PhMe** was prepared *via* the analogous method used for α-**1Cl**. A glass vial containing freshly prepared [MnTBrPP][TCNE]·2PhMe (*ca.* 30 mg) was heated in a tube furnace under dynamic vacuum at 175 °C for 3 h. IR (Nujol; cm^{-1}): ν_{CN} 2201 (m), 2160 (s). Calc. for [MnTBrPP][TCNE] ($C_{50}H_{24}Br_4MnN_8$) *M* 1111.33. C, 54.04; H, 2.18; N, 10.08. Found: C, 54.16; H, 2.22; N, 9.95%.

[MnTBrPP][TCNE]·2CH$_2$Cl$_2$ (1Br·2CH$_2$Cl$_2$). Filtered 10 mL CH_2Cl_2 solutions of Mn^{II}TBrPPpy (57.3 mg, 0.0538 mmol) and TCNE (18.0 mg, 0.140 mmol) were mixed and stirred under nitrogen at room temperature for 4 h**.** The mixture stood for 5 days in an inert atmosphere glovebox. The resulting 30.0 mg of black block crystals were collected by vacuum filtration. IR (Nujol; cm^{-1}): ν_{CN} 2195 (m), 2137 (s).

γ-[MnTBrPP][TCNE] (γ-1Br). The desolvated, γ-**1Br·2CH$_2$Cl$_2$**, was obtained by drying [MnTBrPP][TCNE]·$2CH_2Cl_2$ under reduced pressure for 1 h at room temperature in a 71% yield of shiny black microcrystals. IR (Nujol; cm^{-1}): ν_{CN} 2195 (m), 2137 (s). Calc. for [MnTBrPP][TCNE] ($C_{50}H_{24}Br_4MnN_8$) *M* 1111.33. C, 54.04; H, 2.18; N, 10.08. Found: C, 54.32; H, 2.42; N, 9.56%.

α-[MnTIPP][TCNE] (α-1I). A glass vial containing freshly prepared [MnTIPP][TCNE]·2PhMe (*ca.* 30 mg) was heated in a tube furnace under dynamic vacuum at 175 °C for 3 h (74% yield). IR (Nujol; cm^{-1}): ν_{CN} 2201 (m), 2160 (s).

[MnTIPP][TCNE]·2CH$_2$Cl$_2$ (1I·2CH$_2$Cl$_2$). Filtered 10 mL CH_2Cl_2 solutions of Mn^{II}TIPPpy (81.6 mg, 0.0651 mmol) and TCNE (22.9 mg, 0.191 mmol) were mixed and stirred under nitrogen at room temperature for 4 h. The resulting green plate microcrystals were then collected by vacuum filtration. IR (Nujol; cm^{-1}): ν_{CN} 2202 (m), 2162 (s).

γ-[MnTIPP][TCNE] (γ-1I). The desolvated γ-**1I** was obtained by drying [MnTIPP][TCNE]·$2CH_2Cl_2$ (35.1 mg) under reduced pressure for 1 h at room temperature, yielding 21.3 mg of shiny black microcrystals. IR (Nujol; cm^{-1}): ν_{CN} 2202 (m), 2162 (s), 2124 (vw). Calc. for [MnTIPP][TCNE] ($C_{50}H_{24}I_4MnN_8$) *M* 1299.34. C, 46.22; H, 1.86; N, 8.62. Found: C, 46.37; H, 1.94; N, 8.43%.

Physical methods

The 2 to 300 K dc magnetic susceptibility was determined on a Quantum Design MPMS-5XL 5 T SQUID (sensitivity = 10^{-8} emu or 10^{-12} emu Oe^{-1} at 1 T) magnetometer with an ultra-low field (≈0.005 Oe) option, an ac option enabling the study of the ac magnetic susceptibility (χ' and χ'') in the range of 10 to 1000 Hz, a reciprocating sample measurement system, and continuous low temperature control with enhanced thermometry features. Samples were loaded in gelatin capsules or in airtight Delrin holder and packed with oven-dried quartz wool and excess toluene (to prevent movement of the sample in the holder). For isofield dc measurements, the samples were zero-field cooled (following oscillation of the dc field), and data collected upon warming. For ac measurements, remanant fluxes were minimized by oscillation of the dc field, with the sample cooled in zero applied field with data then taken upon warming. In addition to correcting for the diamagnetic contribution from the sample holder, core diamagnetic corrections of −455, −479, −541, −604, −60, −52 and -47×10^{-6} emu mol^{-1} were used for MnTFPP, MnTClPP, MnTBrPP, MnTIPP, TCNE, PhMe, and CH_2Cl_2, respectively. Infrared spectra (600–4000 ± 1 cm^{-1}) were obtained on a Bio-Rad FT-40 spectrophotometer in mineral oil mulls. Variable temperature IR spectra were obtained in mineral oil mulls in the temperature range of −135 to 180 °C in a homebuilt variable temperature IR cell. The thermal properties were studied on a TA Instruments Model 2050 thermogravimetric analyzer (TGA) equipped with a TA-MS Fison triple filter quadrupole mass spectrometer, to identify gaseous products with masses less than 300 u, located in a Vacuum Atmospheres DriLab under argon. Samples were placed in an aluminum pan and heated at 20 °C min^{-1} under a continuous 10 mL min^{-1} nitrogen flow. Elemental analyses were performed by Atlantic Microlabs, Norcross, GA.

Structure determination of [MnTBrPP][TCNE]·2CH$_2$Cl$_2$

Cell constants and an orientation matrix for the data collection were obtained by the standard methods. Systematic absences and subsequent least-squares refinement were used to determine the space groups. The weighting scheme used was:

$[2\sigma F_o^2]^{-1}$. SHELX-97 was used for the refinement based on the Patterson method with nonhydrogen atoms refined anisotropically.[28] Further refinement/analysis to locate disordered $[TCNE]^{\cdot -}$ was performed through examination of electron density difference maps. Data were also corrected for Lorentz and polarization factors.[29] Disorder in the orientation of $[TCNE]^{\cdot -}$ and solvent were not observed. Empirical absorption corrections were applied. Crystallographic details are summarized in Table 4. The hydrogen atoms were included using the riding model where each H-atom coordinate is re-idealized before each refinement cycle and 'ride' on the atom to which it is attached.

CCDC reference number 186/2048.

See http://www.rsc.org/suppdata/dt/b0/b003458o/ for crystallographic files in .cif format.

Acknowledgements

The authors gratefully acknowledge the support in part from the National Science Foundation Grant Nos. CHE9320478 and CHE9730948. We thank Wendy Hibbs for helpful discussion as well as verifying some data.

References

1 (*a*) C. P. Landee, D. Melville and J. S. Miller, in *NATO ARW Molecular Magnetic Materials*, ed. O. Kahn, D. Gatteschi, J. S. Miller and F. Palacio, 1991, vol. E198, p. 395; (*b*) B. G. Morin, C. Hahm, A. J. Epstein and J. S. Miller, *J. Appl. Phys.*, 1994, **75**, 5782; (*c*) J. S. Miller and A. J. Epstein, *CHEMTECH*, 1991, **21**, 168; (*d*) J. S. Miller, *Adv. Mater.*, 1994, **6**, 322.

2 *Proceedings on the Conference on Ferromagnetic and High Spin Molecular Based Materials*, ed. J. S. Miller and D. A Dougherty, *Mol. Cryst. Liq. Cryst.*, 1989, **176**; *Proceedings on the Conference on Molecular Magnetic Materials*, ed. D. Gatteschi, O. Kahn, J. S. Miller and F. Palacio, *NATO ARW on Molecular Magnetic Materials*, 1991, vol. E198; *Proceedings on the Conference on the Chemistry and Physics of Molecular Based Magnetic Materials*, ed. H. Iwamura and J. S. Miller, *Mol. Cryst. Liq. Cryst.*, 1993, **232/233**; *Proceedings on the Conference on Molecule-based Magnets*, ed. J. S. Miller and A. J. Epstein, *Mol. Cryst. Liq. Cryst.*, 1995, **271**–**274**; *Proceedings on the Conference on Molecular-Based Magnets*, ed. K. Itoh, J. S. Miller and T. Takui, *Mol. Cryst. Liq. Cryst.*, 1997, **305**–**306**; M. M. Turnbull, T. Sugimoto and L. K. Thompson, (Editors), *ACS Symp. Ser.*, 1996, **644**.

3 Reviews; (*a*) V. I. Ovcharenko and R. Z. Sagdeev, *Russ. Chem. Rev.*, 1999, **68**, 345; (*b*) J. S. Miller and A. J. Epstein, *Chem. Commun.*, 1998, 1319; (*c*) W. Plass, *Chem. Ztg.*, 1998, **32**, 323; (*d*) J. S. Miller and A. J. Epstein, *Chem. Eng. News*, 1995, **73**, 30; J. S. Miller and A. J. Epstein, *Angew. Chem., Int. Ed. Engl.*, 1994, **33**, 385; (*e*) M. Kinoshita, *Jpn. J. Appl. Phys.*, 1994, **33**, 5718; (*f*) J. S. Miller and A. J. Epstein, *Adv. Chem. Ser.*, 1995, **245**, 161; (*g*) A. Caneschi, D. Gatteschi and P. Rey, *Prog. Inorg. Chem.*, 1991, **39**, 331; (*h*) A. L. Buchachenko, *Russ. Chem. Rev.*, 1990, **59**, 307; (*i*) O. Kahn, *Struct. Bonding* (*Berlin*), 1987, **68**, 89; (*j*) A. Caneschi, D. Gatteschi, R. Sessoli and P. Rey, *Acc. Chem. Res.*, 1989, **22**, 392; (*k*) D. Gatteschi, *Adv. Mat.*, 1994, **6**, 635; (*l*) J. S. Miller, A. J. Epstein and W. M. Reiff, *Acc. Chem. Res.*, 1988, **21**, 114; (*m*) J. S. Miller, A. J. Epstein and W. M. Reiff, *Science*, 1988, **240**, 40; (*n*) J. S. Miller, A. J. Epstein and W. M. Reiff, *Chem. Rev.*, 1988, **88**, 201; (*o*) J. S. Miller and A. J. Epstein, in *New Aspects of Organic Chemistry*, ed. Z. Yoshida, T. Shiba and Y. Oshiro, VCH Publishers, New York, 1989, p. 237; (*p*) O. Kahn, *Molecular Magnetism*, VCH Publishers, New York, 1993.

4 (*a*) J. S. Miller, J. C. Calabrese, D. A. Dixon, A. J. Epstein, R. W. Bigelow, J. H. Zhang and W. M. Reiff, *J. Am. Chem. Soc.*, 1987, **109**, 769; (*b*) J. S. Miller, J. C. Calabrese, A. J. Epstein, R. W. Bigelow, J. H. Zhang and W. M. Reiff, *J. Chem. Soc., Chem. Commun.*, 1986, 1026; (*c*) S. Chittipeddi, K. R. Cromack, J. S. Miller and A. J. Epstein, *Phys. Rev. Lett.*, 1987, **22**, 2695.

5 (*a*) Y. Pei, M. Verdaguer, O. Kahn, J. Sletten and J. P. Renard, *Inorg. Chem.*, 1987, **26**, 138; (*b*) S. Turner, O. Kahn and L. Rabardel, *J. Am. Chem. Soc.*, 1996, **118**, 6428; (*c*) O. Kahn, Y. Pei, M. Verdaguer, J. P. Renard and J. Sletten, *J. Am. Chem. Soc.*, 1988, **110**, 782; (*d*) K. Nakatani, Y. Carriat, Y. Journaux, O. Kahn, F. Lloret and J. P. Renard, *J. Am. Chem. Soc.*, 1989, **111**, 5739.

6 A. Caneschi, D. Gatteschi, J. P. Renard, P. Rey and R. Sessoli, *Inorg. Chem.*, 1989, **28**, 3314; (*b*) K. Inoue, T. Hayamizu, H. Iwamura, D. Hashizume and Y. Ohashi, *J. Am. Chem. Soc.*, 1996, **118**, 1803.

7 (*a*) J. S. Miller, J. C. Calabrese, R. S. McLean and A. J. Epstein, *J. Adv. Mater.*, 1992, **4**, 498; (*b*) P. Zhou, B. G. Morin, A. J. Epstein, R. S. McLean and J. S. Miller, *J. Appl. Phys.*, 1993, **73**, 6569.

8 (*a*) C. M. Wynn, M. A. Girtu, J. S. Miller and A. J. Epstein, *J. Phys. Rev. B.*, 1997, **56**, 14050; (*b*) C. M. Wynn, M. A. Girtu, K.-i. Sugiura, E. J. Brandon, J. L. Manson, J. S. Miller and A. J. Epstein, *Synth. Met.*, 1997, **85**, 1695; (*c*) C. M. Wynn, M. A. Girtu, J. S. Miller and A. J. Epstein, *Phys. Rev. B*, 1997, **56**, 315; (*d*) A. J. Epstein, C. M. Wynn, W. B. Brinckerhoff and J. S. Miller, *Mol. Cryst. Liq. Cryst.*, 1997, **305**, 321.

9 (*a*) A. Böhm, C. Vazquez, R. S. McLean, J. C. Calabrese, S. E. Kalm, J. L. Manson, A. J. Epstein and J. S. Miller, *Inorg. Chem.*, 1996, **35**, 3083; (*b*) K.-i. Sugiura, A. Arif, D. K. Rittenberg, J. Schweizer, L. Öhrstrom, A. J. Epstein and J. S. Miller, *Chem. Eur. J.*, 1997, **3**, 138; (*c*) E. J. Brandon, K.-i. Sugiura, A. Arif, L. Liable-Sands, A. L. Rheingold and J. S. Miller, *Mol. Cryst. Liq. Cryst.*, 1997, **305**, 269; (*d*) E. J. Brandon, B. M. Burkhart, R. D. Rogers and J. S. Miller, *Chem. Eur. J.*, 1998, **4**, 1938; (*e*) E. J. Brandon, D. K. Rittenberg, A. M. Arif and J. S. Miller, *Inorg. Chem.*, 1998, **37**, 3376; (*f*) E. J. Brandon, A. M. Arif, B. M. Burkhart and J. S. Miller, *Inorg. Chem.*, 1998, **37**, 2792.

10 (*a*) J. S. Miller, C. Vazquez, N. L. Jones, R. S. McLean and A. J. Epstein, *J. Mater. Chem.*, 1995, 5, 707; (*b*) D. K. Rittenberg, K.-i. Sugiura, A. M. Arif, C. D. Incarvito, A. L. Rheingold, Y. Sakata and J. S. Miller, *Chem. Eur. J.*, 2000, **6**, 1811.

11 (*a*) K. Griesar, M. A. Anthanassopoulou, E. A. Soto Bustamante, Z. Tomkowicz, A. J. Zaleski and W. Haase, *Adv. Mater.*, 1997, **9**, 45; (*b*) H. Winter, E. Dormann, R. Gompper, R. Janner, S. Kothrade, B. Wagner and H. Naarmann, *J. Magn. Magn. Mater.*, 1995, **140**–**144**, 1443; (*c*) H. Winter, M. Klemen, W. Dormann, R. Gompper, R. Janner, S. Kothrade and B. Wagner, *Mol. Cryst. Liq. Cryst.*, 1995, **273**, 111; K. Falk, R. Werner, Z. Tomkowicz, M. Belanda and W. Haase, *J. Magn. Magn. Mater.*, 1999, **196**–**197**, 564; M. Belanda, K. Falk, K. Griesar, Z. Tomkowicz and W. Haase, *J. Magn. Magn. Mater.*, 1999, **205**, 14; M. Belanda, K. Falk, K. Griesar, Z. Tomkowicz, T. Wasiutynski and W. Haase, *Mol. Cryst. Liq. Cryst.*, 1999, **335**, 133.

12 E. J. Brandon, A. M. Arif, J. S. Miller and B. M. Burkhart, *Cryst. Eng.*, 1998, **1**, 97. J. S. Miller and E. J. Brandon, in *NATO ARW Supramolecular Engineering of Synthetic Metallic Materials: Conductors and Magnets*, ed. J. Veciana, C. Rovira, D. Amabilino, 1998, vol. C518, p. 197.

13 I. Goldberg, H. Krupitsky, Z. Stein, Y. Hsiou and C. E. Strouse, *Supramol. Chem.*, 1995, **4**, 203; H. Krupitsky, Z. Stein and I. Goldberg, *J. Inclusion Phenom. Mol. Recognit.*, 1995, **20**, 211; I. Goldberg, *Mol. Cryst. Liq. Cryst.*, 1996, **278**, 767; M. P. Byrn, C. J. Curtis, Y. Hsiou, S. I. Kahn, P. A. Sawin, S. K. Tendick, A. Terzis and C. E. Strouse, *J. Am. Chem. Soc.*, 1993, **115**, 9480.

14 D. K. Rittenberg and J. S. Miller, *Inorg. Chem.*, 1999, **38**, 1746.

15 D. A. Dixon and J. S. Miller, *J. Am. Chem. Soc.*, 1987, **109**, 3656.

16 Crystal data for $[MnTClPP][TCNE]\cdot 2CH_2Cl_2$:[9e] $C_{52}H_{28}N_8MnCl_8$, $M = 1103.42$, monoclinic, $a = 9.894(2)$, $b = 10.697(2)$, $c = 23.560(5)$, $\beta = 101.34(2)°$, $Z = 2$, $V = 2444.6(8)$ Å^3, $T = 225$ K, space group = $P2_1/n$, λ(Mo-K$_\alpha$) = 0.71073 Å, $R(F_o) = 0.0411$, $wR(F_o) = 0.1034$.

17 (*a*) V. W. Day, B. R. Sults, E. L. Tasset, R. S. Marianelli and L. J Boucher, *Inorg. Nucl. Chem. Lett.*, 1975, **11**, 505; (*b*) B. Cheng, F. Cukiernik, P. Fries, J.-C. Marchon and W. R. Scheidt, *Inorg. Chem.*, 1995, **34**, 4627; (*c*) R. Guildard, K. Perie, J.-M. Barbe, D. J Nurco, K. M. Smith, E. V Caemebecke and K. M. Kadish, *Inorg. Chem.*, 1998, **37**, 973.

18 D. K. Rittenberg, K.-i. Sugiura, Y. Sakata, I. A. Guzei, A. L. Rheingold and J. S. Miller, *Chem. Eur. J.*, 1999, **5**, 1647.

19 J. Seiden, *J. Phys. Lett.*, 1983, **44**, L947.

20 M. Drillion, E. Coronado, R. Georges, J. C. Gianduazzo and J. Curely, *J. Phys. Rev. B*, 1989, **40**, 10992.

21 A. Bencini and D. Gatteschi, *EPR of Exchange Coupled Systems*, Springer-Verlag, New York, 1989.

22 E. J. Brandon, C. Kollmar and J. S. Miller, *J. Am. Chem. Soc.*, 1998, **120**, 1822.

23 J. A. Mydosh, *Spin Glasses*, Francois and Taylor, Washington, DC, 1993.

24 J. L. Manson and J. S. Miller, unpublished work.

25 D. C. Mattis, *The Theory of Magnetism*, Springer-Verlag, New York, 1981, vol. 1.

26 D. K. Rittenberg, K.-i. Sugiura, A. M. Arif, Y. Sakata and J. S. Miller, *Adv. Mater.*, 2000, **10**, 126.

27 A. D. Alder, F. R. Longo, J. D. Finarelli, J. Goldmacher and L. Korsakoff, *J. Org. Chem.*, 1967, **32**, 476.
28 G. M. Sheldrick, SHELX97-2, Programs for Crystal Structure Analysis (Release 97-2), Universität Göttingen, Germany, 1998.
29 Using the program CHAIN [J. S. Sack, *J. Mol. Graphics*, 1988, **6**, 224] on a graphics workstation evidence for disorder of the cation, anion and solvent was sought without success: B. M. Burkhart, personal communication.
30 C. K. Johnson, Report ORNL-5138, Oak Ridge National Laboratory, Oak Ridge, TN, 1976.